

PECULIAR MID-INFRARED MORPHOLOGY OF ACTIVE GALACTIC NUCLEUS IN CIRCINUS

M. STALEVSKI¹, D. ASMUS² and K. R. W. TRISTRAM²

¹*Astronomical Observatory, Volgina 7, 11060 Belgrade, Serbia*
E-mail: mstalevski@aob.rs

²*European Souther Observatory, Casilla 19001, Santiago 19, Chile*

Abstract. Recent high angular resolution observations resolved for the first time the mid-infrared (MIR) structure of nearby active galactic nuclei (AGN). Surprisingly, they revealed that a major fraction of their MIR emission comes from the polar regions. This is at odds with the expectation based on AGN unification, which postulates a dusty torus in the equatorial region. The nearby, archetypical AGN in the Circinus galaxy offers one of the best opportunities to study the MIR emission in greater detail. New, high quality MIR images obtained with the upgraded VISIR instrument at the Very Large Telescope show that the previously detected bar-like structure extends up to at least 40 pc on both sides of the nucleus along the edges of the ionization cone. Motivated by observations across a wide wavelength range and on different spatial scales, we propose a phenomenological dust emission model for the AGN in the Circinus galaxy consisting of a compact dusty disk and a large-scale dusty cone shell, illuminated by a tilted accretion disk with an anisotropic emission pattern. Undertaking detailed radiative transfer simulations, we demonstrate that such a model is able to explain the peculiar MIR morphology and account for the entire IR spectral energy distribution. Our results call for caution when attributing dust emission of unresolved sources entirely to the torus and warrant further investigation of the MIR emission in the polar regions of AGN.

1. INTRODUCTION

During the lifetime of a galactic nucleus, the supermassive black hole (SMBH) in its center may accrete significant amounts of matter at a relatively high rate. This phenomenon, known as an active galactic nucleus (AGN), manifests itself through a number of energetic phenomena such as: a compact X-ray source, a strong UV/optical continuum, a number of broad and/or narrow emission lines, a radio-jet, to name a few. Approximately half of the luminosity radiated by the matter spiraling onto the SMBH in an accretion disk is absorbed by the surrounding dust and reemitted in the infrared (IR). The distribution of dust and the viewing angle determine how an AGN appears to an observer as they combine to reveal or hide the accretion disk and broad line region (AGN type 1 and type 2, respectively; see Antonucci, 1993). This dusty material, postulated to be found preferentially in the equatorial plane of the system and roughly in a toroidal shape, has been rooted in AGN jargon as “the dusty torus”, even though a number of both theoretical and observational pieces of evidence suggest that it is more likely to resemble a complex multiphase medium, possibly associated to

dusty outflows or failed winds. A bulk of observational evidence has been accumulated over the years in support of this scenario (Netzer, 2015).

Owing to their small angular sizes, only with recent advances of IR interferometry several nearby sources could be resolved, surprising revealing that the mid-infrared (MIR) emission of these sources appears elongated in the polar direction, perpendicular to the plane of the dusty torus (Lopez-Gonzaga et al. 2016 and references therein). Extended MIR polar emission was detected even in single dish data on the scales of tens to hundreds of parsecs, virtually in all sources with sufficient S/N data and favorable viewing angle (Asmus et al. 2016). These findings challenge the use of standard dusty torus models to interpret the IR emission and demand a new paradigm for the dust structure in AGN. Crucial steps towards the new paradigm are case studies of nearby objects that can be resolved and studied extensively across a broad range of wavelengths. One such object is the archetypal type 2 AGN at the distance of 4.2 Mpc in the Circinus galaxy. Being the second brightest AGN in the MIR and allowing high intrinsic spatial resolution ($1'' = 20$ pc), Circinus is a prime target for a large number of studies across a wide wavelength range. These observations revealed a number of features expected from a prototypical type 2 AGN. [OIII] and $H\alpha$ emission reveal the ionization cone on the West side (Wilson et al. 2000); the East cone is covered by the host galaxy disk but was detected in polarized near-infrared light (Ruiz et al. 2000). Water maser emission traces a near-Keplerian, warped disk seen edge-on (Greenhill et al. 2003). A bar-like extended emission at was detected at 8.7 and $18.3\ \mu\text{m}$ extending up to $\sim 2''$ from each side of the nucleus, roughly in east-west direction. Modeling of the MIR interferometric data obtained with the MID-infrared Interferometric instrument (MIDI) at the Very Large Telescope Interferometer (VLTI) reveals two components on parsec-scale: a disk-like component in the equatorial plane of the system, and a larger structure elongated in the polar direction (Tristram et al. 2007, Tristram et al. 2014). The disk-like component is likely a molecular, dusty extension of the accretion disk. Furthermore, it well matches the orientation and scale of the warped maser disk. The association of the polar-extended component is less clear. It could be the inner wall of the torus, which then would need to have a very large scale height, or it could be the base of a polar dusty wind, which is forming a large cone shell.

The upgraded Imager and Spectrometer for mid-Infrared (VISIR) mounted on the Very Large Telescope (VLT) provided up-to-date highest quality MIR images of Circinus. These images show a previously detected, prominent bar extending 40 pc on both sides of the unresolved nucleus. This bar cannot be explained by the torus: it is aligned with the polar component inferred by interferometric data and with the edge of the ionization cone seen at optical wavelengths. In this work we proposed a model for dust emitting regions of AGN in Circinus that may explain this puzzling finding.

2. OBSERVATIONS

We selected the highest quality MIR data available for Circinus. In particular, two new images at $8.6\ \mu\text{m}$ and $11.9\ \mu\text{m}$ (Fig. 1, top left panel) were obtained with the upgraded VISIR¹, allowing us to achieve diffraction-limited image quality. We complement them with archival VISIR images in the filters ($10.5\ \mu\text{m}$) and Q2 ($18.7\ \mu\text{m}$) tracing the two

¹Program ID 60.A-9629

silicate features at ~ 10 and $\sim 18 \mu\text{m}$ (Fig. 2). Here, we simply take the reduced data from Asmus et al. (2014) and refer the reader to that work for more details on these data. Resolved emission in the form of a bar stretching out from the center at a position angle of roughly 100° both to the East and West is revealed. This emission structure is well visible at all four wavelengths out to ~ 40 pc on both sides, and coincides with the edge of the ionization cone seen at visible wavelengths on the Western side. For comparison of the model and the data over a wider wavelength range, we also assemble the observed nuclear SED and spectra of Circinus from data available in the literature. Finally, we also include so far unpublished L -band data² from VLT/ISAAC to obtain a contemporary estimate for the $3.8 \mu\text{m}$ flux.

3. MODEL

The large scale MIR bar (extending up to 40 pc on both sides of the nucleus) seen by VISIR is aligned with the polar-elongated component on parsec-scale, suggesting that both are part of the same physical structure. The big surprise is that this structure is dominating the MIR emission: $\sim 10\%$ of the total flux in the MIR is coming from the disk-like component ($\sim 0.2 - 1.1$ pc), about 40-50% from the parsec-scale polar component ($\sim 0.8 - 1.9$ pc), and another 40-50% from the large-scale polar bar (Tristram et al. 2014; Asmus et al. 2016). On the other hand, if the large-scale polar bar is part of a hollow dusty cone, one would expect this cone to appear as an X-shaped structure. Hence the question arises: why the other side of the cone wall does not appear in the VISIR images? *Our hypothesis is that the inner accretion disk is significantly tilted (and/or warped) so that it preferentially illuminates only one side of the dusty cone wall.* This picture is supported by the orientation of the inner part of the warped water maser disk and by the anisotropic illumination pattern imprinted in the ionization cone. In Fig. 1, we present a schematic of our model that has the potential to explain the MIR bar seen with VISIR, and at the same time fits well into the picture placed by the previous observations at different wavelengths, both on small and large scales. The overall geometry is well constrained by observations: a parsec-scale dusty disk, co-spatial with the warped maser disk seen edge-on (upper right panel), and an ionization cone seen in the optical, extending out to ~ 40 pc from the nucleus (lower right panel). The illumination pattern of the ionization cone (brighter toward the western edge) is indicative of the anisotropic emission pattern of the ionizing source. This is corroborated by the orientation of the inner part of the maser disk, which is roughly perpendicular to the cone edge. An optically-thick, geometrically-thin accretion disk displays a $\cos \theta$ angular-dependent luminosity profile (Stalevski et al. 2016). Aligned with the inner part of the warped maser disk, such a disk will emit more strongly into or close to the western edge of the cone. If the cone wall is dusty, then the described setup could naturally produce the dusty bar seen in the VISIR image. The opposite side of the cone wall would remain cold and invisible, as the tilted anisotropic accretion disk would emit very little in that direction (see temperature profile in the lower left panel).

In a summary, the model consists of two components whose parameters take fiducial values implied by the different observations discussed above: a compact flared dusty disk and a hollow dusty cone. The accretion disk, described by a standard

²Programmes 385.B-0896(B), 386.B-0026(B), 087.B-0746(B), 088.B-0159(B), 089.B-0070(B)

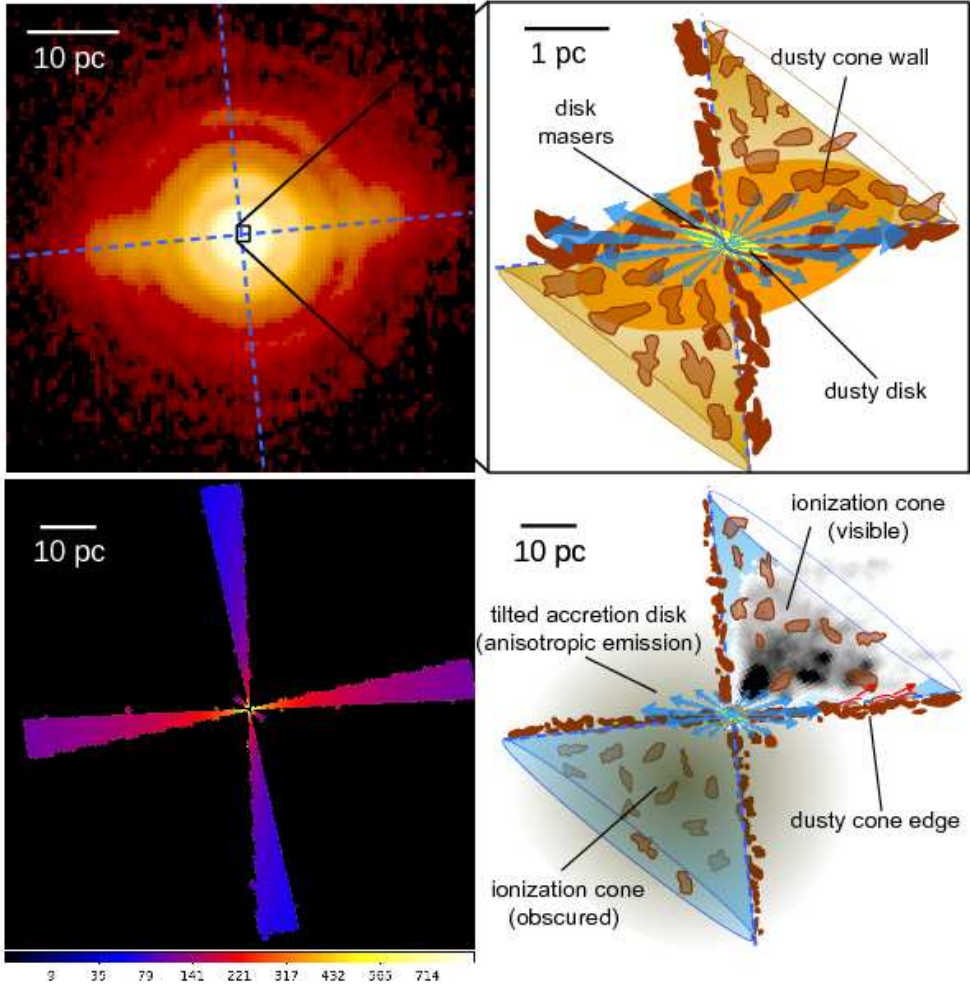


Figure 1: Schematic of the model proposed here for the nuclear dust distribution in Circinus consisting of a compact dusty disk and a large scale dusty cone, compared with observations at different wavelengths and scales. *Upper left panel:* $12\ \mu\text{m}$ VLT/VISIR image revealing the prominent bar. *Upper right panel:* inner region on scales of a few parsecs resolved by VLT/MIDI into the disk and polar components (yellow and orange ellipsoids). The red line within the yellow disk component traces the warped disk in water maser emission (Greenhill et al., 2003). *Lower right panel:* The large scale structure, with the optical ionization cone image (from Wilson et al., 2000; in gray scale) overlaid with the model schematic. The blue arrows illustrate the anisotropic emission pattern of the accretion disk, whose orientation matches the orientation of the inner part of the warped maser disk. Dashed blue lines in all the panels are tracing the edges of the ionization cone. *Lower left panel:* A slice of the temperature map in the vertical plane of the disk with cone model obtained from Monte Carlo radiative transfer simulations.

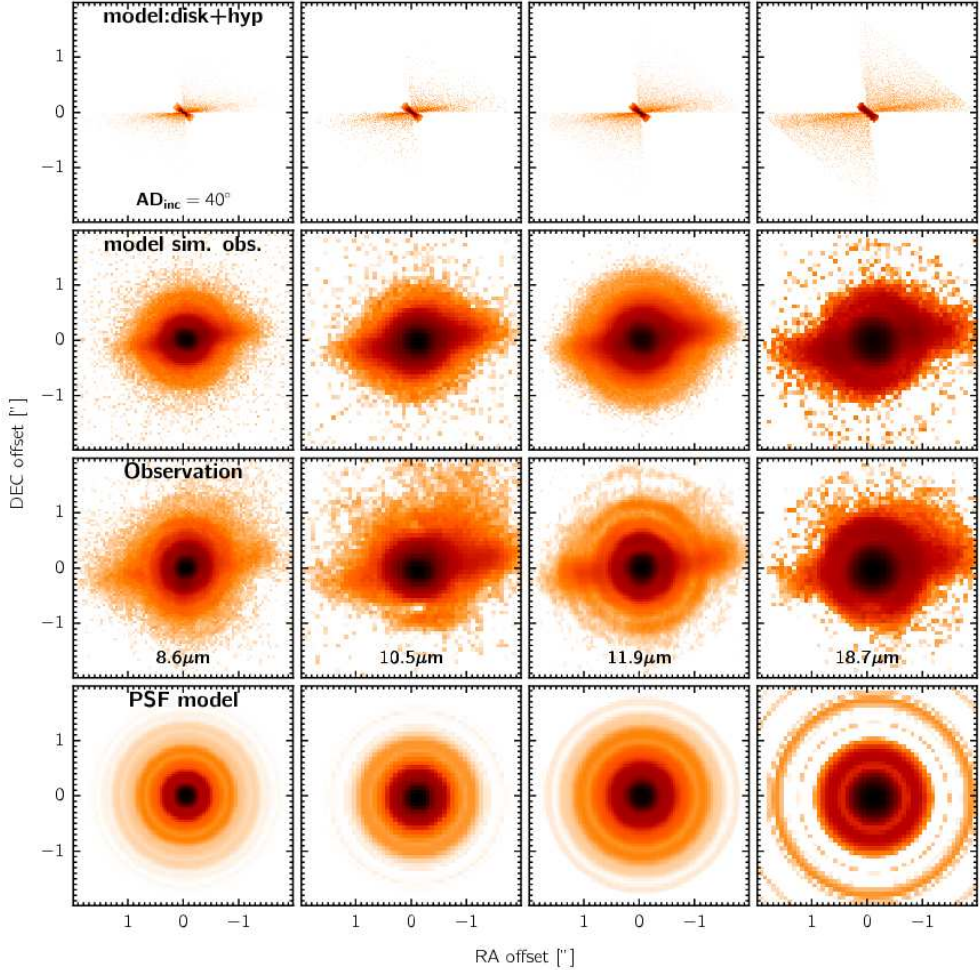


Figure 2: Comparison of the VISIR images of Circinus with the representative model (whose SED is shown in Fig. 3), including foreground extinction. From top to bottom, the rows show: (1) the model images; (2) the model images as they would appear when observed with VISIR; (3) the images of Circinus acquired with VISIR; (4) our approximation of the observed PSF.

“blue bump” composition of power-laws with an anisotropic emission pattern, is tilted to match the orientation of the inner part of the warped maser disk. We adopt the dust composition consisting of a mixture of graphite and silicates in the disk and only graphite in the cone shell. The dust grain size is in the range of $a = 0.1 - 1 \mu\text{m}$ with the size distribution following the standard MRN power-law $\propto a^{-3.5}$ (Mathis, Rumpl & Nordsieck 1977). For a full description of the model and its parameters, see Stalevski et al. (2017).

4. RESULTS

To obtain realistic images and SEDs for the proposed model, we employed SKIRT³, a state-of-the-art 3D radiative transfer code based on the Monte Carlo technique (Baes et al. 2011; Baes & Camps, 2015; Camps & Baes, 2015). The code uses the Monte Carlo technique to emulate the relevant physical processes including multiple anisotropic scattering and absorption, and computes the temperature distribution of the dust and the thermal dust re-emission self-consistently. In Fig. 3, we show the AGN in Circinus galaxy model SED decomposed into its scattered and dust emission

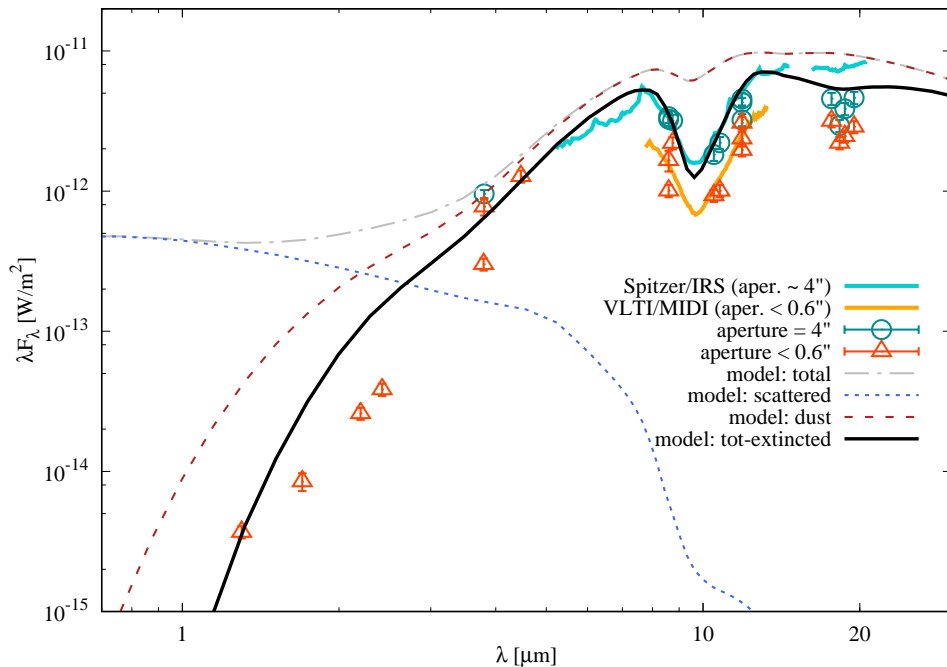


Figure 3: AGN in Circinus galaxy: comparison of the observed SED compiled from the literature with one representative model SED. Large-scale aperture photometry ($4''$) is shown in green circles, while photometry extracted from apertures comparable or smaller than the resolution limit of VISIR ($0.6''$) is marked by red up-pointing triangles. The measurement uncertainties are smaller or comparable to the plotted symbol size. The aperture of the Spitzer/IRS spectrum from Asmus et al. (2014) is comparable to the total aperture of VISIR in the $5.2 - 14.5 \mu\text{m}$ range, while significantly larger at longer wavelengths. The MIDI spectrum from Tristram et al. (2014) corresponds to the unresolved nucleus with VISIR. The model SED is decomposed into its total (dash-dotted gray), scattered (dotted blue) and dust (dashed dark red) components. For a realistic comparison, foreground absorption must be taken into account: the total model flux extinguished by foreground screen of average $\tau_{9.7} = 1.6$ is shown in solid black line.

³<http://www.skirt.ugent.be>

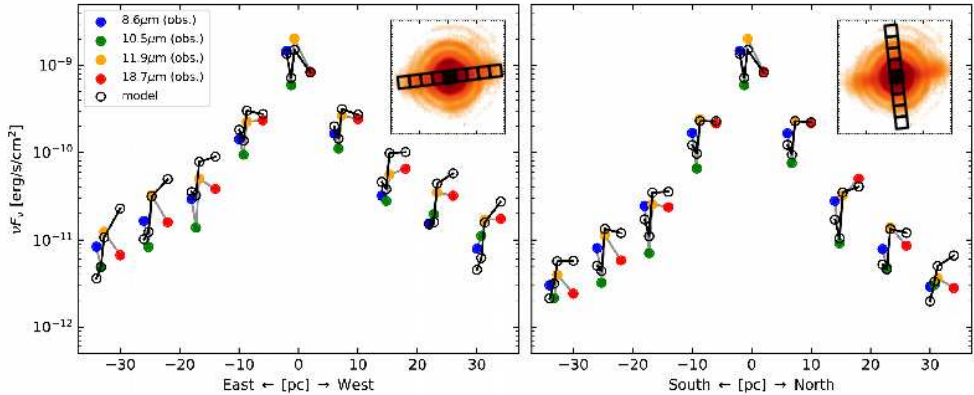


Figure 4: Comparison of observed and model photometry (from images shown in Fig. 2) extracted in $0.4'' \times 0.4''$ aperture fields in the directions along the bar (left) and perpendicular to it (right), as indicated in the inset plots. The central position corresponds to the unresolved nucleus.

components, and attenuated by dust of the host galaxy. We see that scattered light has a significant contribution shortward of $3 \mu\text{m}$; however, it is completely extinguished by the foreground dust screen. The model SED has a weak silicate absorption feature, which becomes much deeper and matches the data after the foreground extinction screen is applied. We note that there are models featuring silicate absorption profiles that could fit the data with much less or without the foreground extinction screen. However, foreground absorption is robustly established by the very deep off-center optical depth values (Roche et al. 2006), and we consider realistic only those models which provide a good match including the inferred amount of extinction. In Fig. 2, we compare the VISIR images of Circinus with the simulated observations of our representative model, including background noise and foreground extinction. Since the observations are diffraction-limited, we include in the plot the instrumental PSF, approximated by an azimuthally symmetric structure of the reference star, to allow easier interpretation of the images. We see that the simulated model images provide a good match to the observed morphology in all filters. We compare the VISIR images and the simulated observations of the model in more detail in Fig. 4 by measuring fluxes at different positions extracted from $0.4'' \times 0.4''$ apertures along the MIR bar and perpendicular to it. An overall qualitatively good agreement is evident, especially at the central position and close to it. All the presented comparison and analysis is leading us to conclude that the here presented model consisting of a compact dusty disk and large scale dusty cone shell illuminated by a tilted accretion disk with anisotropic emission pattern plausibly represents the actual dust structure in Circinus.

5. SUMMARY AND CONCLUSIONS

Recent findings of significant MIR emission in the polar regions of local AGN challenge the widely accepted picture in which the parsec-sized “torus” is responsible for the entire AGN dust emission and may demand a change of paradigm. One of the sources showing clear polar extended dust is the archetypal type 2 AGN in the Circinus

galaxy. Up-to-date highest quality images obtained with the upgraded VLT/VISIR instrument feature a prominent bar extending in the polar direction of the system. In this work, we presented a phenomenological model for the dust emitting regions in this source consisting of a compact dusty disk and a large scale dusty hollow cone region illuminated by a tilted accretion disk with anisotropic emission. The model is supported by observations across a range of different wavelengths and spatial scales. Using Monte Carlo radiative transfer simulations we produced the images and SEDs of this model. Based on the comparison with the observed MIR morphology and the measured SED we find that the model of the polar dust in the form of a hollow cone is able to reproduce the observed MIR morphology at all wavelengths. Furthermore, the model provides a good match to the entire IR SED of Circinus, including resolved photometry extracted from apertures at different positions along the polar bar and perpendicular to it. We conclude that our model consisting of a compact dusty disk with a large scale dusty cone shell is plausibly a good representation of the dust structure of the AGN in the Circinus galaxy. Our results call for caution when attributing thermal dust emission of unresolved sources entirely to the torus and warrant further investigation, including detailed modeling of other sources showing polar elongation of their MIR emission as well as developing a theoretical framework that would explain the origin of the dust in the polar regions. Our model of the AGN in Circinus can be used as a prototype and as a guideline for such studies. Full investigation with more detailed analysis, including a wider range of the model parameters and different geometries, can be found in Stalevski et al. (2017).

References

- Antonucci, R.: 1993, *ARA&A*, **31**, 473.
Asmus, D., Hönic, S. F., Gandhi, P., Smette, A., Duschl, W. J.: 2014, *MNRAS*, **439**, 1648.
Asmus, D., Hönic, S. F., Gandhi, P.: 2016, *ApJ*, **822**, 109.
Baes, M., Verstappen, J., De Looze, I. et al.: 2011, *ApJS*, **196**, 22.
Baes, M., Camps, P.: 2015, *A&C*, **12**, 33.
Camps, P., Baes, M.: 2015, *A&C*, **9**, 20.
Greenhill, L. J., Booth, R. S., Ellingsen, S. P. et al.: 2003, *ApJ*, **590**, 162.
Lopez-Gonzaga, N., Burtscher, L., Tristram, K. R. W. et al.: 2016, *A&A*, **591**, A47.
Mathis, J. S., Rumpl, W., Nordsieck, K. H.: 1977, *ApJ*, **217**, 425.
Netzer, H.: 2015, *ARA&A*, **53**, 365-408.
Roche, P. F., Packham, C., Telesco, C. M. et al.: 2006, *MNRAS*, **367**, 1689.
Ruiz, M., Alexander, D. M., Young, S. et al.: 2000, *MNRAS*, **316**, 49.
Stalevski, M., Ricci, C., Ueda, Y. et al.: 2016, *MNRAS*, **458**, 2288.
Stalevski, M., Asmus, D., Tristram, K. R. W.: 2017, *MNRAS*, **472**, 3854.
Tristram, K. R. W., Meisenheimer, K., Jaffe, W. et al.: 2007, *A&A*, **474**, 837.
Tristram, K. R. W., Burtscher, L., Jaffe, W. et al.: 2014, *A&A*, **563**, A82.
Wilson, A. S., Shopbell, P. L., Simpson, C. et al.: 2000, *AJ*, **120**, 1325.